SEM ANALYSIS OF BOND EPOXY BASED LAYER BETWEEN HARDENED CONCRETE AND SFRC REPAIRING

E. Bonaldo[a], J.P. Castro-Gomes[b], J. A. O. Barros[c], P. B. Lourenço[d]

a. *PhD Student, University of Minho, Department of Civil Engineering, School of Engineering, Guimarães, Portugal, bona@civil.uminho.pt*

b. *Associate Professor, University of Beira Interior, Department of Civil Engineering and Architecture, castro.gomes@ubi.pt*

c. *Associate Professor, University of Minho, Department of Civil Engineering, School of Engineering, Guimarães, Portugal, barros@civil.uminho.pt*

d. *Associate Professor, University of Minho, Department of Civil Engineering, School of Engineering, Guimarães, Portugal, pbl@civil.uminho.pt*

Abstract

Thin bonded concrete overlay are commonly used nowadays in repairing concrete structures. Nevertheless, the performance of the structural system (repaired structure) depends on the sound bond behaviour between old and new concretes. Frequently, adhesives based on epoxy resins provide this liaison. In this work the behaviour of three different types of based epoxy adhesives was observed in the bonding of different strength concrete class. Samples for backscattered scanning electron microscopy (BSE) were prepared from extracted pieces - containing the bonding layer - of non reinforced concrete slabs overlaid with thin bonded steel fibre reinforced concrete (SFRC) layer. Different features of each bonding layer epoxy resin type which may explain differentiate mechanical pull-off results as well as failure modes were observed. Micrographs obtained with BSE give clearly bond layer arrangement and minimum and maximum thickness, typical air voids porosity, presence of hydrated cement paste embedded in epoxy layer, mineral admixtures contained in epoxy, and also relevant micro fissures existing in concrete substrate.

Keywords: epoxy adhesive, concrete repairing, steel fibre reinforced concrete, imaging analysis, bond layer microstructure.

Introduction

The present work deals with aspects related to the microstructural analysis of the bond between concrete of distinct characteristics, and is a part of a more comprehensive research project involving carbon fibre reinforced polymer (CFRP) and discrete steel fibres for flexural strengthening and rehabilitation of concrete slabs. In the hybrid strengthening (see Figure 1) strategy, to overcome the limitation (concrete crushing in the compression region) resulted from the CFRP strengthening, a thin layer of steel fibre reinforced concrete (SFRC) can be bonded to the existing concrete at the compression surface, using an adhesive compound (Barros & Sena-Cruz, 2001). The development and maintenance of a sound bond between the overlay and the existing concrete substrate is an utmost requirement for the performance of the strengthening. Epoxy based resins cured at room temperature are easy to apply and since unaffected by water-saturated system of fresh concrete can provide appropriated adhesion between hardened and fresh concrete.

The aim of this work is to examine microstructural attributes information of the bond layer using BSE analysis of specimen polished surfaces. As well know presently, cement and concrete properties - mainly compressive strength - can be directly predicted based on miscrostructure info (Garboczi et al., 2004). Thus, another goal of the present study is to provide a better understanding of the bonding mechanisms (hardened concrete - epoxy adhesive - fresh SFRC), connecting observed characteristics of the images of the bonding layer system in between the concretes and experimental bond behaviour assessed using pull-off testing.

Different microscopy features of each epoxy resin are identified. These differences in microstructure are in accordance with corresponding mechanical pull-off results as well as failure modes. Microscopy images obtained with BSE analysis give clearly bond layer arrangement and thickness boundary, typical air voids porosity, presence of hydrated cement paste embedded in epoxy layer, mineral admixtures contained in epoxy, and also relevant micro fissures existing in concrete substrate. Thus, it is believed that the analysis of bond layer microstructure, presented in this work, contributes to a better understanding of mechanical pull-off results.

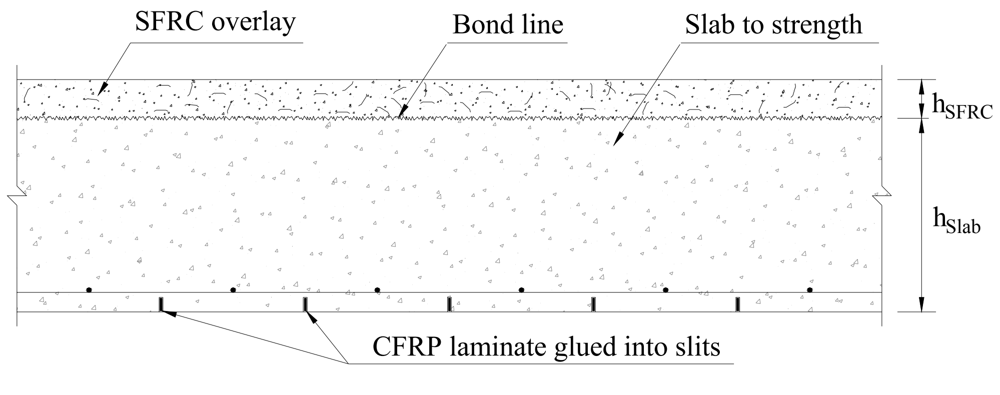

Figure 1: The hybrid strengthening technique for concrete slabs: CFRP laminate in tension zone and bonded SFRC overlay in compression zone.

Materials and Bonding Properties

Details concerning the materials used in the present work, main bonding procedures and bonding strength follows.

Concrete Substrate and SFRC Overlay

The experimental campaign was composed by three main series, each one with a distinct concrete strength class for the substrate. Each of this series was composed by two series of two different concrete strength classes for the overlay, resulting in a total of six series, as indicated in Table 1. The concrete overlay was always reinforced with Hooked ends DRAMIX® RC-80/60-BN steel fibres (Dramix, 1998).

Table 1: Target concrete strength classes of the tests.

Concrete substrate (ordinary concrete)	**Concrete overlay** (with steel fibres)
C16/20	C20/25 C25/30
C35/45	C35/45 C45/55
C55/67	C55/67 C60/75

The average compressive strength of the ordinary concrete (substrate) and SFRC overlay achieve from 3 cylinder specimens (150 mm in diameter and 300 mm in height) at 28 days of age is shown in Table 2.

Table 2: Concrete base and SFRC overlay compressive strength (in MPa).

Base	**B1**		**B2**		**B3**	
(ordinary concrete)	22.32		42.59		60.82	
Overlay (SFRC)	**C1**	**C2**	**C3**	**C4**	**C5**	**C6**
	25.87	32.08	41.50	53.51	62.54	66.81
	C1’	**C2’**		**C3’**	**C4’**	**C5’**
	27.36	38.48		58.46	66.67	64.50

Bond Agents

Three types of epoxy-based bond agents were selected to bond fresh SFRC overlay to hardened concrete substrate, namely two epoxy resin-based products (P1 and P2), and one epoxy resin and cement-based product (P3). Table 3 and 4 show some summarized information about the bond products.

The time necessary for grinding a portion of hardened resin into a fine powder using a ball mill, provides additional information about the bond products hardness. Using a Retsch ball mil at about 30 revolutions per second (1800 RPM), 1 minute was enough for grinding a quantity of about 500 mg of bond resin P1 and P3. Whereas 10 minutes was necessary for grinding the same bond resin P2 portion (Nunes, 2003).

The bond coating materials were applied onto dry and clean concrete, i.e., free from surface contaminants such as dust, laitance, oil or grease, according with the manufacturer. Consumptions of 2.26, 0.90 and 3.17 kg/m^2 were used for bond product P1, P2 and P3, respectively.

Table 3: Data extracted from commercial datasheet for the bond products (Sika, 2002).

Bond	**Commercial designation**	**Specific gravity**	***Pot life* / open time at 20 °C**
P1	Icosit® K 101	≈ 1.8 kg/l	45 min / 90 min
P2	Sikadur® 32 N	≈ 1.4 kg/l	≈ 25 min/ 3 h
P3	Sikatop® Armatec 110 EpoCem®	≈ (at 20ºC) A+B+C mix 2.0 kg/l	1.5 h (at 30 °C)/ 12 h

Table 4: Mechanical properties of the bond products (Sika, 2002).

Bond	**Bond strength**	**Mechanical resistance**
P1	to concrete: ~3 MPa (concrete failure) to sandblasted steel: ~20 MPa	Compressive strength: ~90 MPa Flexural strength: ~45 MPa
P2	to concrete: 2.5 - 3.0 MPa (concrete failure) to sandblasted steel: 18 - 20 MPa	Compressive strength: ~60 - 70 MPa Tensile strength: ~18 - 20 MPa Flexural strength: ~30 - 35 MPa
P3	to sandblasted concrete: 2 - 3 MPa to steel: 1 - 2 MPa	-

Main Bonding Procedures

Nonreinforced concrete slabs of 300 mm x 650 mm, with 80 mm thickness, were used as concrete substrate. When the concrete substrate attained 28 days of age, the top surface of the slab specimen was treated. The bond product was then applied and the freshly concrete overlay was cast. For the aims of this research, an overlay thickness of approximately 30 mm of SFRC layer was adopted.

A specimen before surface treatment and the equipment used to roughen the surface is shown in Figure 2.

The process of roughening the top surface of the concrete substrate had the purpose of removing a very thin layer of the surface, in order to remove grease, oils, free particles, laitance or dirt, as well as producing an irregular surface. Figure 3 shows the main bond steps. When the concrete overlay attained an age of about 28 days, the partial core was drilled and the pull-off tests were carried out.

Bonding Strength

The mechanical bond behaviour was assessed from pull-off tests on non reinforced substrate concrete slabs overlaid with SFRC. The series of tests were composed according to the concrete strength given in Table 2. The influence of the strength class of concrete substrate and repairing SFRC, and also the adhesive agent used to bond the two concretes was analysed (Bonaldo et al., 2004). The mechanical resistance - pull-off strength, is summarized in Figure 4. For a more comprehensive review refer to Bonaldo et al. (2004, 2005).

(a) *(b)*

Figure 2: The specimen surface before roughening (a) and the roughening machine (b).

(a) *(b)* *(c)*

Figure 3: Main steps of the bonding process of the SFRC overlay: (a) placing the bond product, (b) consolidating of the SFRC and (c) curing with wet burlap.

Bond Layer Microstructural Characteristics

Figure 5 to 10 present BSE micrographs of the bond layer of different epoxy resins P1, P2 and P3 for low and high strength concrete classes. In these micrographs the bottom horizontal part corresponds to concrete substrate, while the top part corresponds to SFRC overlay; layer of epoxy resin is visible in between.

Specimens Preparation for BSE Study

Concrete specimens for microscopy study were prepared from extracted pieces (approximately 15 mm specimens size) containing the bonding layer of non reinforced concrete slabs overlaid with bonded thin steel fibre reinforced concrete (SFRC) layer. The extracted concrete pieces of about two years old were impregnated with an epoxy resin obtained from Struers, surface finer polished and carbon coated. Small pieces of Epoxy resins P1, P2 and P3, were also impregnated with Struers resin and prepared in the same manner as the concrete specimens for BSE microscopy. The specimens preparation procedures adopted herein are complying with the specimens preparation described in detail elsewhere (Bentz & Stutzman, 1994).

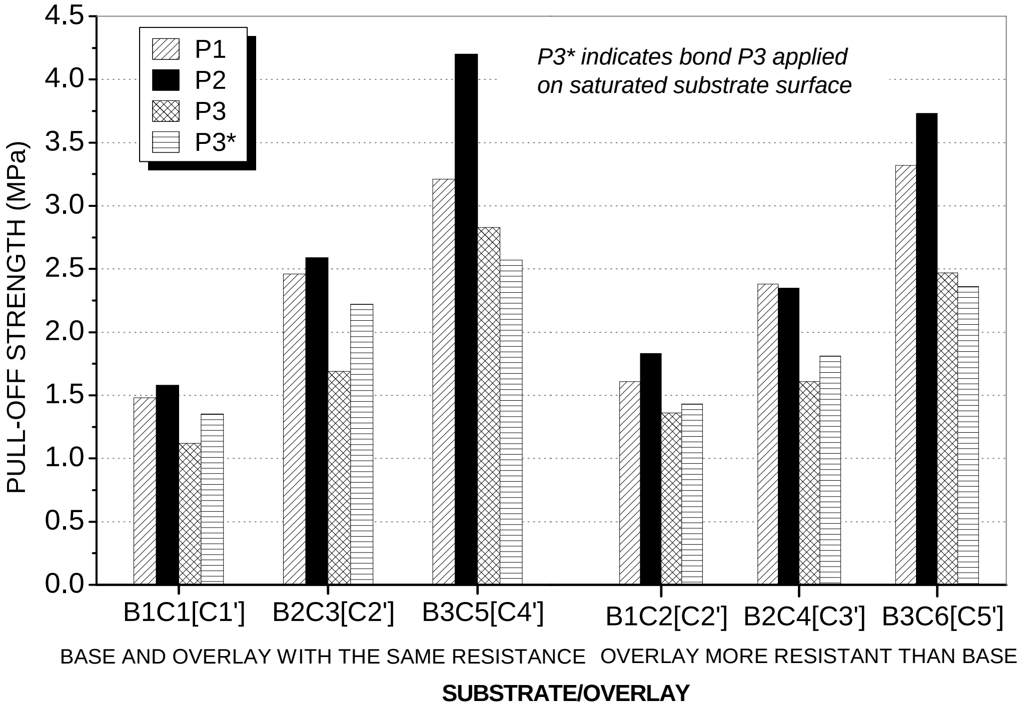

Figure 4: Pull-off average strength for each substrate and overlay type. Here $B_nC_m[C_m']$ indicates: B_n - ordinary concrete substrate, C_m - SFRC overlay bonded with P1, P2 and P3, and $[C_m']$ - SFRC overlay bonded with P3, on saturated substrate surface ($P3^*$).

Bonding Layer with Epoxy P1

Micrographs of sample bond system B1-P1-C1 and B3-P1-C5 are presented in Figures 5 and 6, respectively. These images show a well defined boundary line corresponding to base concrete, connected to the epoxy layer. The top layer corresponding to SFRC does not have a well defined boundary line. On the contrary, SFRC sand particles and hydrate cement paste are intercalated in the epoxy resin layer. The sand particles are of size between 0.3 and 0.5 mm approximately, and hydrate cement paste varies from very small individual particles to clusters of about 300 μm diameter.

The epoxy layer bond in Figure 5 has about 1 mm mean value thickness, and also contains a large amount of a mineral admixture (white entities). Thus giving this layer different characteristics from bottom to top which may be considered as three distinct sub-layers as follows: close to boundary substrate bottom line there is high concentration of mineral admixture blended in epoxy, in the middle portion the resin layer has sand particles and hydrate cement clusters and, in the top sub-layer, fragments of epoxy resin are mixed together with hardened SFRC.

Porosity is also visible in the bond layer, resulting from air voids with sizes ranging from about 5 to about 20 μm.

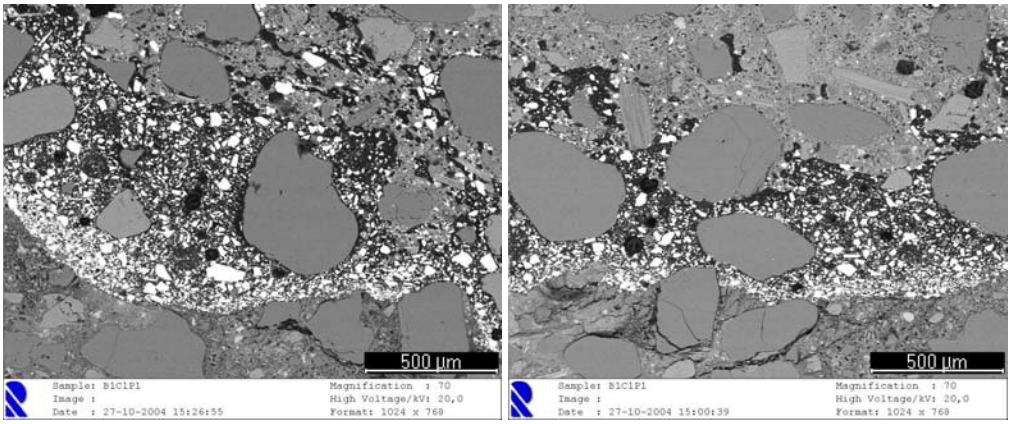

(a)Bond Layer P1 (70x mag.) *(b) Bond Layer P1 (70x mag.)*

Figure 5: Micrographs of sample bond system B1-P1-C1.

Micrographs of bond system B3-P1-C5, presented in Figure 6, exhibit very small differences from those of B1-P1-C1 system. However, in this case it seams that the mineral admixtures of epoxy resin are more evenly distributed. The epoxy bond layer is well defined and also contains sand particles and hydrated cement clusters embedded with it.

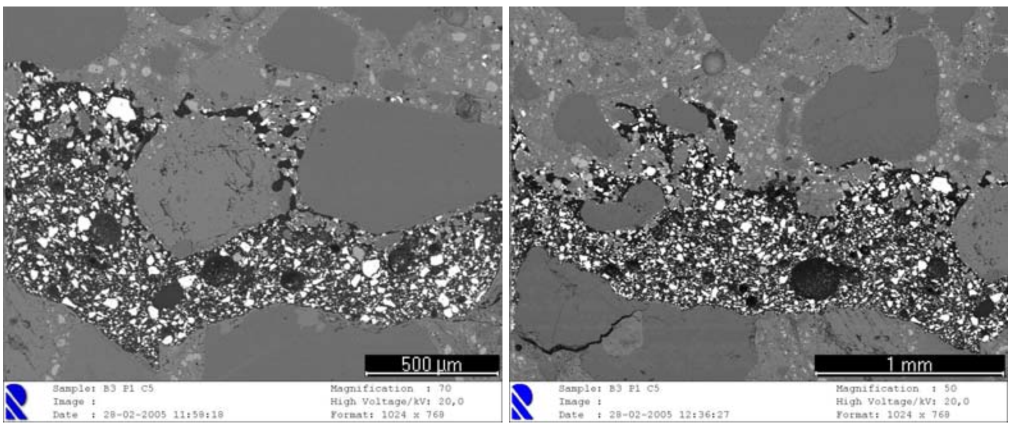

(a) Bond Layer P1 (70x mag.) *(b)Bond Layer P1 (50x mag.)*

Figure 6: Micrographs of sample bond system B3-P1-C5.

In Figure 7 (a) a steel fibber completely embedded in resin bond layer is shown.

Characteristics of Epoxy P1

Figure 7 (b) presents the resin epoxy bond layer at 200x magnification. EDX analysis was done in points 1, 2, 3 and 4 identified in this figure. Point 2 corresponds to a cement particle partially hydrated, as commonly found in hardened cement pastes (Castro-Gomes et al., 1998), and point 3 corresponds to a small sand particle.

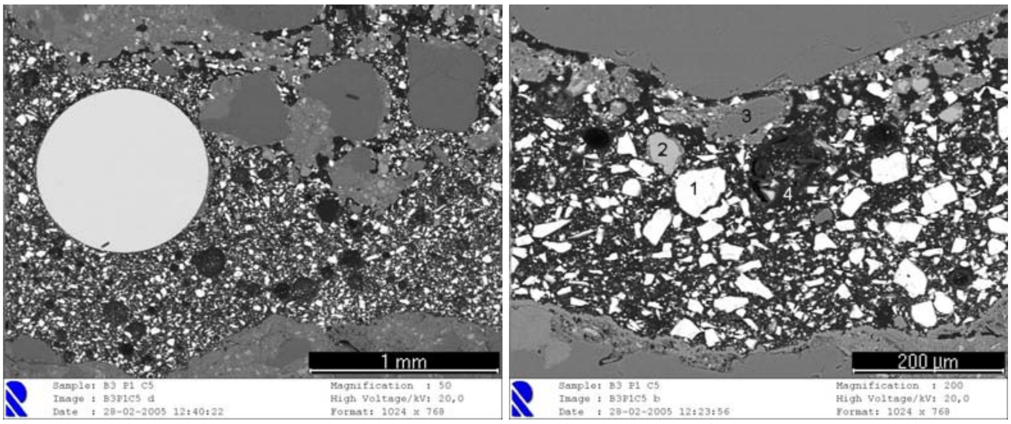

(a)Bond Layer P1 (50x mag.) *(b)Bond Layer P1 (200x mag.)*

Figure 7: Micrographs of sample bond system B3-P1-C5.

The features of concrete microstructure observed with BSE image analysis are in accordance with features found by others (Diamond and Bonen, 1995; Marchand et al., 1996; Diamond, 2004; and Scrivener, 2004).

The points 1 and 4 of Figure 7 (b) correspond to the bright clusters and dark areas, respectively, which constitute the resin bond layer. The bright clusters correspond to the mineral admixture while the dark areas are the epoxy resin itself. This was confirmed with the EDX analysis in points 1 and 4.

The EDX analysis of point 1 is presented in Figure 8 (c). It shows that the mineral admixture is most probably crushed fragments of barite ($BaSO_4$), although this information was not supplied by the producer. The morphology of these particles is sharply angular and exhibit conchoidal fracture, as expected in crushed fragments of barite. Some particles are elongated, some are prismatic, and other particles are thin and thick tabular.

Figures 8 (a) and (b) shows micrographs of epoxy resin P1 at two different magnifications. These micrographs also show that resin P1 contains another mineral admixture appearing light grey, which is not barite that appears bright white.

The EDX of Figure 8 (d) corresponds to this other mineral, particularly the light grey cluster visible in the micrograph of Figure 8 (b). The EDX gives presence of Mg and Ca elements which indicates that it might correspond to a magnesium clay, such as magnesium dolomite (Mg, Ca) CO_3. According to the supplier it corresponds to a variety of montmorillonite clay. It is known that modified clays are very fine materials commonly used blended with epoxy resins to modify its thixotropic properties. Other fine materials like cristobalite, fine quartz, fumed silica or fine barite particles can also be used with the same purpose. These colloidal fine materials are thixotropic agents. They increase resin viscosity when it is in contact with absorbing materials, for example, such us concrete, thus preventing resin to be absorbed in concrete pores.

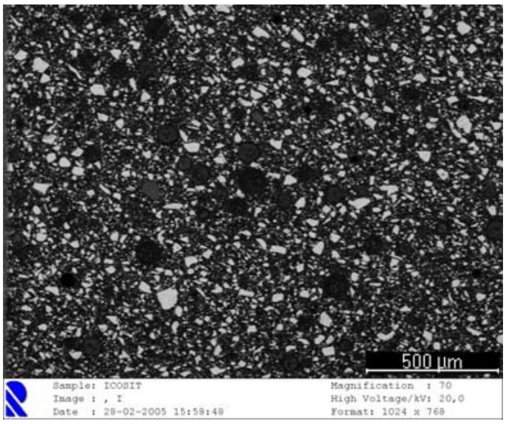

(a) Epoxy Resin P1 (70x mag.)

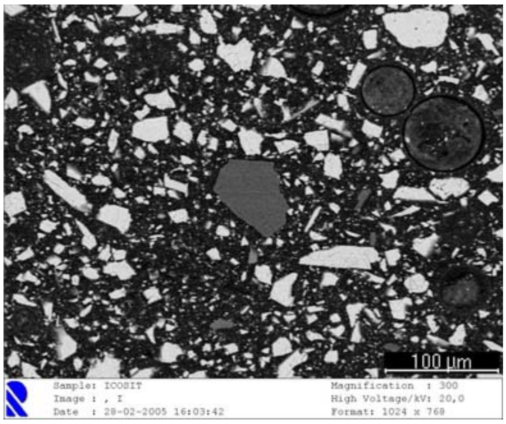

(b) Epoxy Resin P1 (300x mag.)

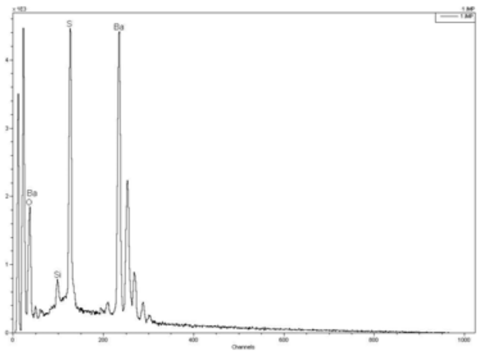

(c) EDX of point 1 (Figure 7(a))

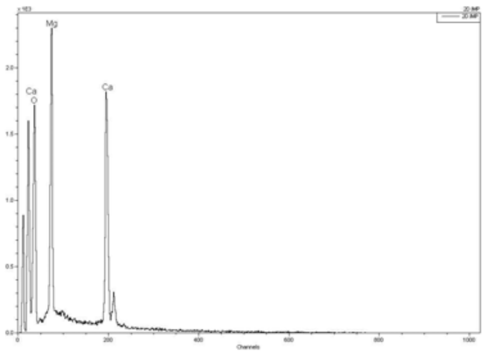

(d) EDX of grey cluster (Figure 8 (b))

Figure 8: Micrographs and EDX graphs of epoxy resin P1.

Bonding Layer with Epoxy P2

Figures 9 and 10, present sample bond system B1-P2-C1 and B3-P2-C5, respectively. The first micrograph of Figure 9 (a) shows epoxy layer thickness varying from 0.5 mm to 1 mm. Figure 9 (b) shows a bond layer with thickness up to 2.5 mm. The top concrete layer is somewhat intercalated with the resin layer, as in the case systems of low strength concrete with epoxy P1. However, in case of P2 resin, it seems that larger cement paste clusters of those found in systems with epoxy P1 were involved with the resin. This apparently results from the fact that the epoxy compound P2 is denser than P1, as was found during the application in the laboratory.

Some sand particles of the overlay are also found embedded in the epoxy resin layer. According to the producer, resin P2 contains 25 - 50% quartz filler (SiO_2), clearly visible and relatively well distributed, although with some concentration in the low portion of the bond layer in system B1-P2-C1. Some porosity resulting from air voids of 50 to about 100 μm is also visible.

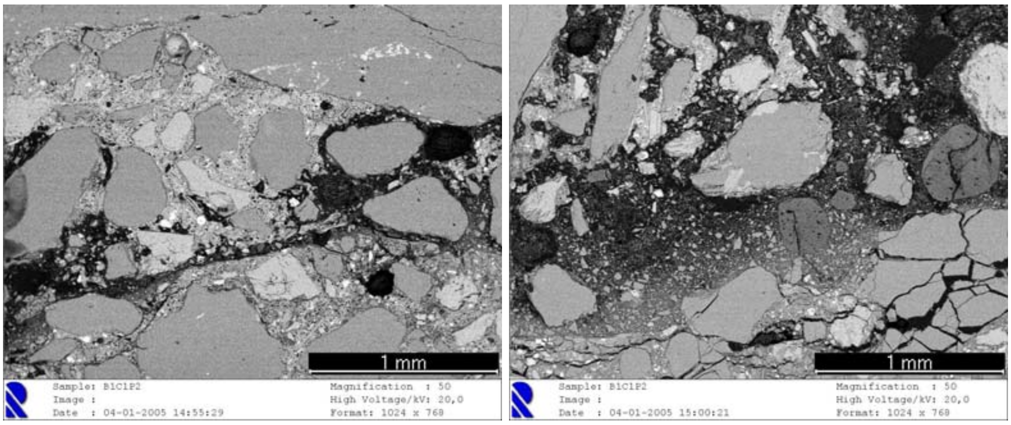

(a) Bond Layer P2 (50x mag.) *(b) Bond Layer P2 (50x mag.)*

Figure 9: Micrographs of sample bond system B1-P2-C1.

Micrographs of Figure 10 show similar features of epoxy region bond system B3-P2-C5. In this case the epoxy bond layer contour appears better defined than in system B1-P2-C1. Similar well defined epoxy layer contour was found in system B3-P1-C5. Concrete top and bottom layers of B3-P2-C5 system show reasonable amount of anhydrous cement and partially hydrated cement particles. It is well known that in cases of low water cement ratios significant amounts of partially hydrated and anhydrous cement can still be found in hardened concrete, even after one year age (Castro-Gomes et al. 1998).

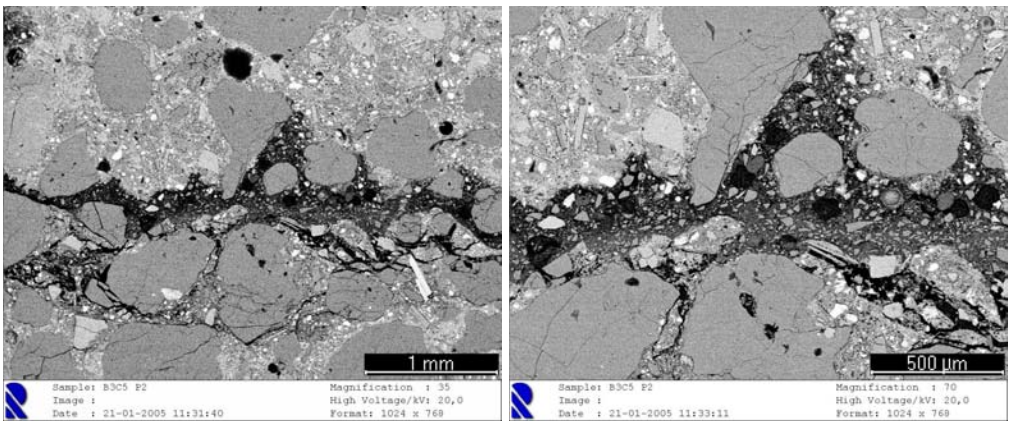

(a) Bond Layer P2 (35x mag.) *(b) Bond Layer P2 (70x mag.)*

Figure 10: Micrographs of sample bond system B3-P2-C5.

Characteristics of Epoxy P2

Figures 11 (a) and (b) presents resin epoxy P2 at two different magnifications. EDX analysis was done in points 1 and 2 identified in Figure 11 (b). EDX graphs of points 1 and 2 are presented in Figures 11 (c) and (d), respectively. According to EDX analysis, white particles were identified as quartz (SiO_2). This is in accordance with producer information given. The morphology of quartz is identical to the morphology of barite, found in resin P1. However, the percentage of quartz particles found in P2 resin is smaller than barite particles percentage blended in P1 resin. This is evident when comparing micrographs of Figures 8 (b) and 11 (b). It is also evident that both quartz and barite particles are of very fine or colloidal degree and are smaller than approximately 80 μm.

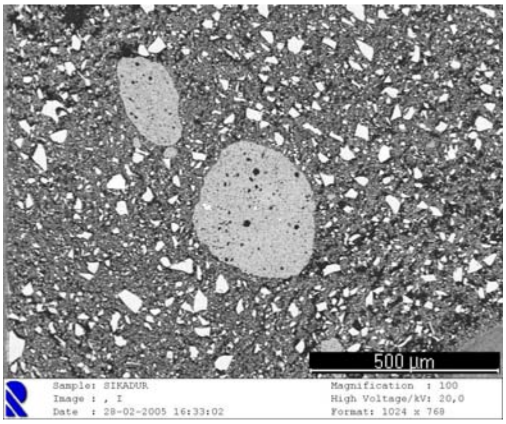

(a)Epoxy Resin P2 (100x mag.)

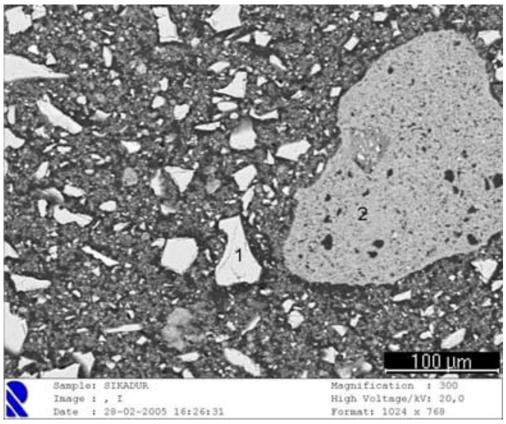

(b)Epoxy Resin P2 (300x mag.)

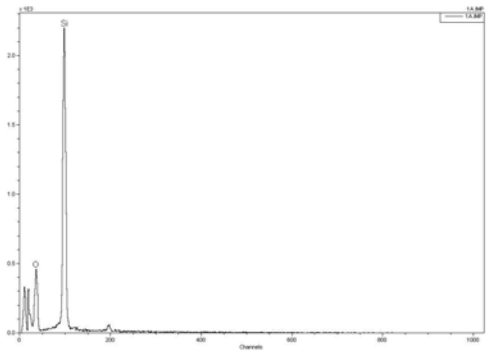

(c)EDX of white particles (Figure 11(a))

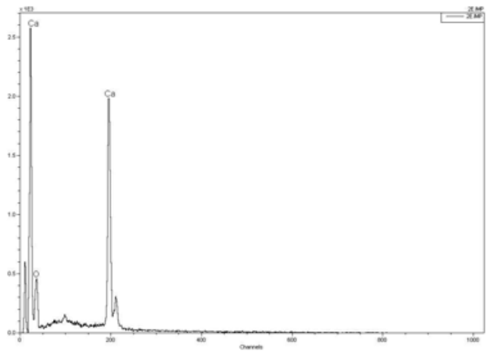

(d)EDX of grey cluster (Figure 11 (b))

Figure 11: Micrographs and EDX graphs of epoxy resin P2.

EDX in point 2 (the large light grey particle) gives mainly calcium. This indicates that the other mineral admixture is calcite $CaCO_3$, as was confirmed by the manufacturer. However this regular shaped fragments could correspond to dolomite..

Bonding Layer with Epoxy P3

Micrographs of sample bond system B1-P3-C1 are presented in Figure 12. This image shows the epoxy layer of about 2 mm thickness (from 1 mm up to 3 mm). The boundaries are not easily identified as in P1 and P2 previous micrographs. Sand particles and mortar of the top layer are uniformly blended with the epoxy cement layer and apparently there are no separately clusters as in P1 and P2 bonds. Finer porosity, 2 or 3 μm as well as void pores of 20 to 30 μm are visible. A significant amount of anhydrous cement and partially hydrated cement in the bond layer is also clearly noticeable.

Micrographs of sample bond system B3-P3-C5 are given in Figure 13 and show similar features of those found in Figure 12.

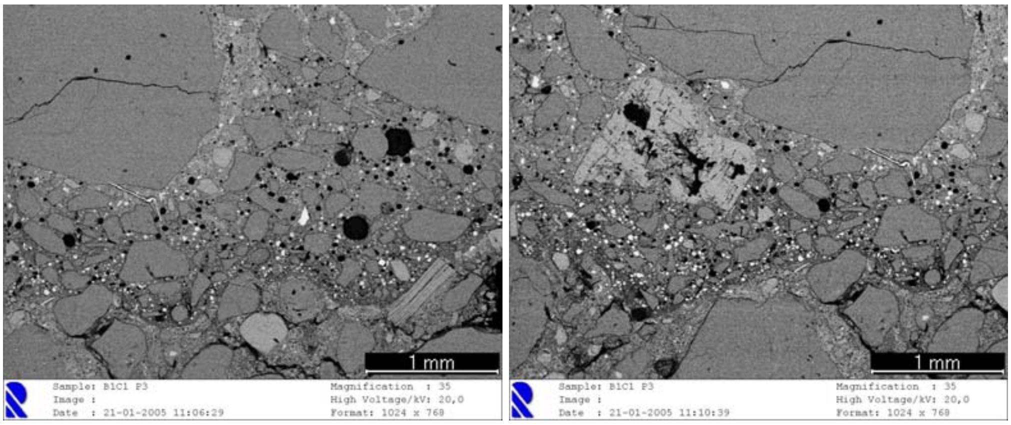

(a) Bond Layer P3 (35x mag.) *(b) Bond Layer P3 (35x mag.)*

Figure 12: Micrographs of sample bond system: B1-P3-C1.

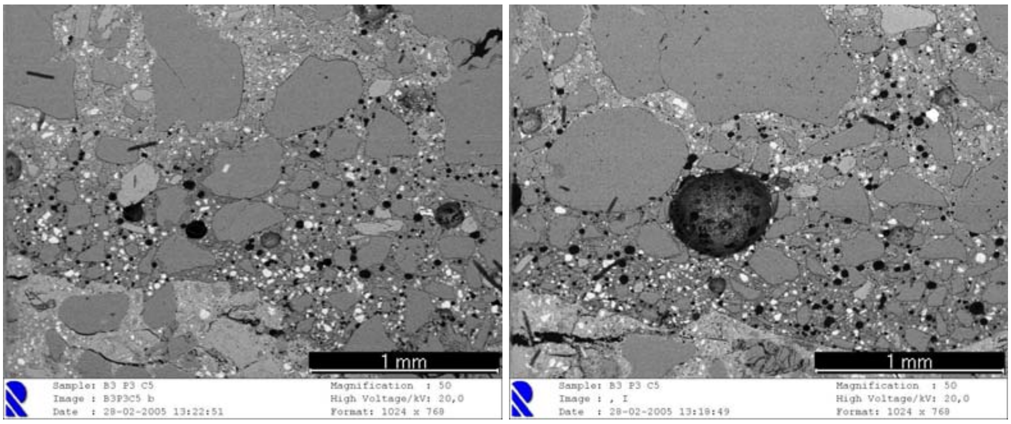

(a) Bond Layer P3 (35x mag.) *(b) Bond Layer P3 (35x mag.)*

Figure 13: Micrographs of sample bond system: B3-P3-C5.

Characteristics of Epoxy P3

EDX analysis and micrographs of resin P3 are presented in Figure 14. According to EDX spectrum in point 1, grey particles were identified as fine sand quartz (SiO_2) while grey particles corresponding to point 2 are identified as partially hydrated cement. This is as expected according with resin producer information.

Quartz sand particles size varies from 0.1 to 0.5 mm.

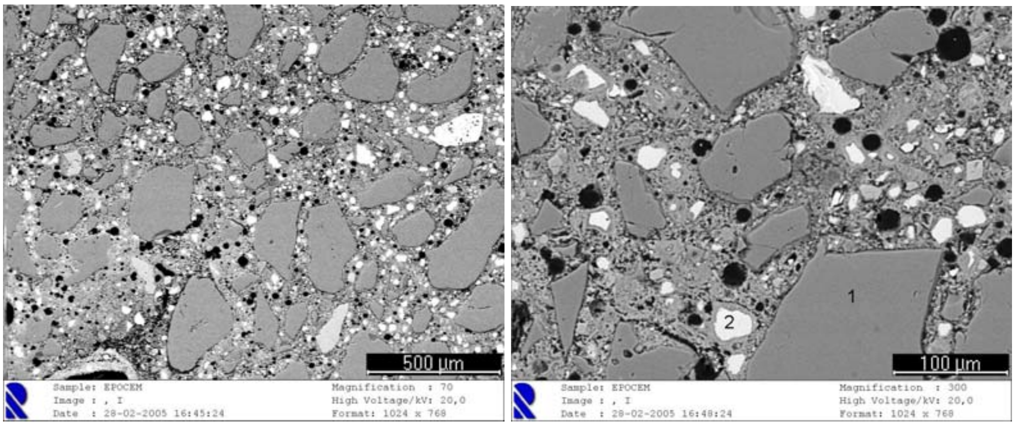

(a) Epoxy Resin P3 (100x mag.) *(b) Epoxy Resin P3 (300x mag.)*

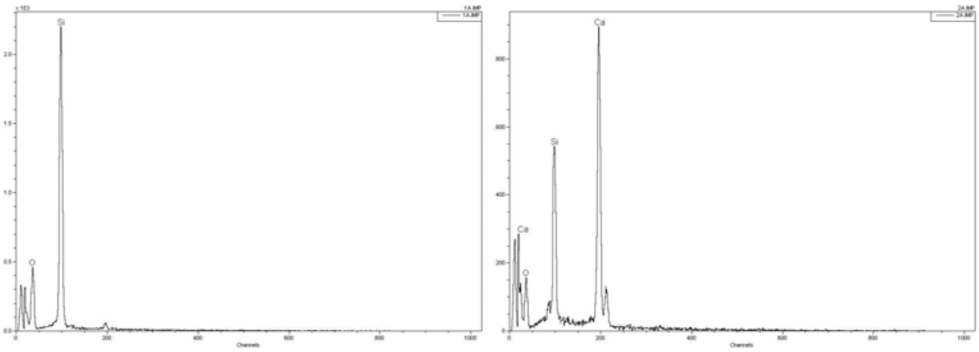

(c) EDX of white particles (Figure 14 (b)) *(d) EDX of grey particles (Figure 14 (b))*

Figure 14: Micrographs and EDX graphs of epoxy resin P3.

Microcracks in Concrete Substrate

In the previous micrographs, microcracks are observed in the concrete substrate. The microcracking phenomenon extends to about 1 mm into the concrete substrate and is associated to the surface treatment used (see Figure 2).

Conclusions

The aim of the present paper is to give some microscopic information on the bonding frontier of fresh SFRC overlay bonded to hardened concrete substrate with epoxy resin. Micrographs obtained using BSE technique revealed some important features of the architecture of the bond layer system which can be useful to explain the bond behaviour mechanism when linked to experimental behaviour.

The analysis of the failure modes recorded in the pull-off test, on SFRC overlay bonded with three commercially available bond agents, denoted as P1, P2 and P3, revealed the pull-off strengths and failure modes are greatly influenced by the bond material type and strength of the concrete substrate (Bonaldo et al., 2004, 2005). The P2 bond material attained greater average pull-off strengths than the others bond materials, independently of the substrate and overlay strength.

For bond material P3 all concrete substrate series showed failure surfaces located in the bond-substrate concrete interface and in the bond product layer. The porosity, anhydrous cement and partially hydrated cement particles and also the low strength of P3 material can explain this type of failure.

For the case of the bond materials P1 and P2, a tendency of the failure surface to move upwards (direction of the fresh concrete overlay) was observed with increasing the substrate strength. For the low strength concrete substrate failures located in a region which is far from the bond line were verified. On the contrary, the fracture surface was located in the base near the bonding layer and in some cases has reached it and also went further into the SFRC overlay, for the case of medium and high strength concrete substrate. As the failure develops in a tortuous mode at the fragile parts, such failure behaviour is likely due to the fact that the failure started at the microcracked part, moved to the weak parts of the bonding layer and/or SFRC overlay (void pores). The higher strength of bond material P2, and also the clusters presence in the bonding layer, can justify the high pull-off strength attained with this material.

Acknowledgements

The first author acknowledges the financial support of the Portuguese Science and Technology Foundation (FCT), PhD grant number SFRH / BD / 11232 / 2002. Thanks also for the companies Sika S.A., "Companhia Geral de Cal e Cimento S.A. (SECIL)", Degussa Construction Chemicals Portugal S.A., "Pedreiras Bezerras", Bekaert NV, which generously have supplied epoxy bond products and its composition, cement, superplasticizer, aggregates, and steel fibres, respectively

References

Barros, J.A.O., and Sena-Cruz, J.M. (2001): Strengthening a prestressed concrete slab by epoxy-bonded FRP composites and SFRC overlayer. Proceedings of the 7th International Conference on Inspection Appraisal Repairs & Maintenance of Buildings & Structures, Nottingham Trent University, UK, pp. 11 - 13 September.

Bentz, D.P., and Stutzman, P.E. (1994): Petrography of cementitious materials, ASTM STP 1215, Sharon M. DeHayes and David Stark, Eds., American Society for Testing and Materials, Philadelphia, pp. 60 - 73.

Bonaldo, E., Barros, J.A.O., and Lourenço, P. B. (2004): Bond characterization between concrete base and repairing SFRC by pull-off tests, Report 04-DEC/E-13, University of Minho, Portugal, May, 57 pp.

Bonaldo, E., Barros, J.A.O., and Lourenço, P. B. (2005): Bond characterization between concrete substrate and repairing SFRC using pull-off testing, International Journal of Adhesion & Adhesives, article in press.

Castro-Gomes, J.P., Cabrera, J.G. and Jalali, S. (1998): The Degree of Cement Hydration Determined by Backscattered Electron Imaging, Proceedings of The Materials Science and Engineering of Concrete and Cementitious-Based Composites Symposium, Aug-Sept, Hawaii, pp. 109 - 126.

Diamond, S. and Bonen, D. (1995): A re-evaluation of hardened cement paste microstructure based on backscatter SEM investigations. In: Diamond S., Mindess S., Glasser F.P., Roberts L.W., Skalny J.P., Wakeley L.D., editors. Microstructure of cement based systems/bonding and interfaces in cementitious materials. Proceedings of the Materials Research Society Symposium, vol. 370. pp. 13 - 22.

Diamond, S. (2004): The microstructure of cement paste and concrete - a visual primer, Cement and Concrete Composites, 26 (8): pp. 919 - 933.

Dramix (1998): Product data sheet, N. V. Bekaert S.A.

Garboczi, E.J., Bullard, J.W., and Bentz, D.P. (2004): Virtual testing of cement and concrete - USA 2004, Concrete International, 26 (12): pp. 33 - 34.

Marchand, J., Hornain, H., Diamond, S., Pigeon, M. and Guiraud, H. (1996): The microstructure of dry concrete products, Cement and Concrete Research, 26 (3): pp. 427 - 438.

Nunes, T.G. (2003): Caracterização de amostras de resinas epoxídicas por espectroscopia de ressonância magnética nuclear de ^{13}C de estado sólido, com a técnica CP-DD/MAS (Characterization of epoxy resins samples by CP/DD/MAS Carbon-13 NMR spectroscopy), Private Report, IST, Portugal, December, 10 pp. (in Portuguese)

Scrivener, K.L. (2004): Backscattered electron imaging of cementitious microstructures: understanding and quantification, Cement and Concrete Composites, 26 (8): pp. 935 - 945.

Sika (2002): Technical data sheet - construction, Sika, S.A., 434 pp. (in Portuguese)